Structure, Volume *30*

Supplemental Information

How insulin-like growth factor I binds to a hybrid insulin receptor type 1 insulin-like growth factor receptor

Yibin Xu, Mai B. Margetts, Hari Venugopal, John G. Menting, Nicholas S. Kirk, Tristan I. Croll, Carlie Delaine, Briony E. Forbes, and Michael C. Lawrence

Figure S1. Protein sequences of the two constructs use to form HybZip, Related to STAR Methods.

(**A**) IR-Bzip, comprising residues 1-928 of the human IR-B isoform followed by the 33-residue GCN4 zipper sequence (*orange*).

(**B**) IGF-1Rzip, comprising residues 1-905 of human IGF-1R followed by the 33-residue GCN4 zipper sequence (*orange*) followed by a three-serine spacer and the c-myc tag sequence EQKLISEEDLN (*blue*).

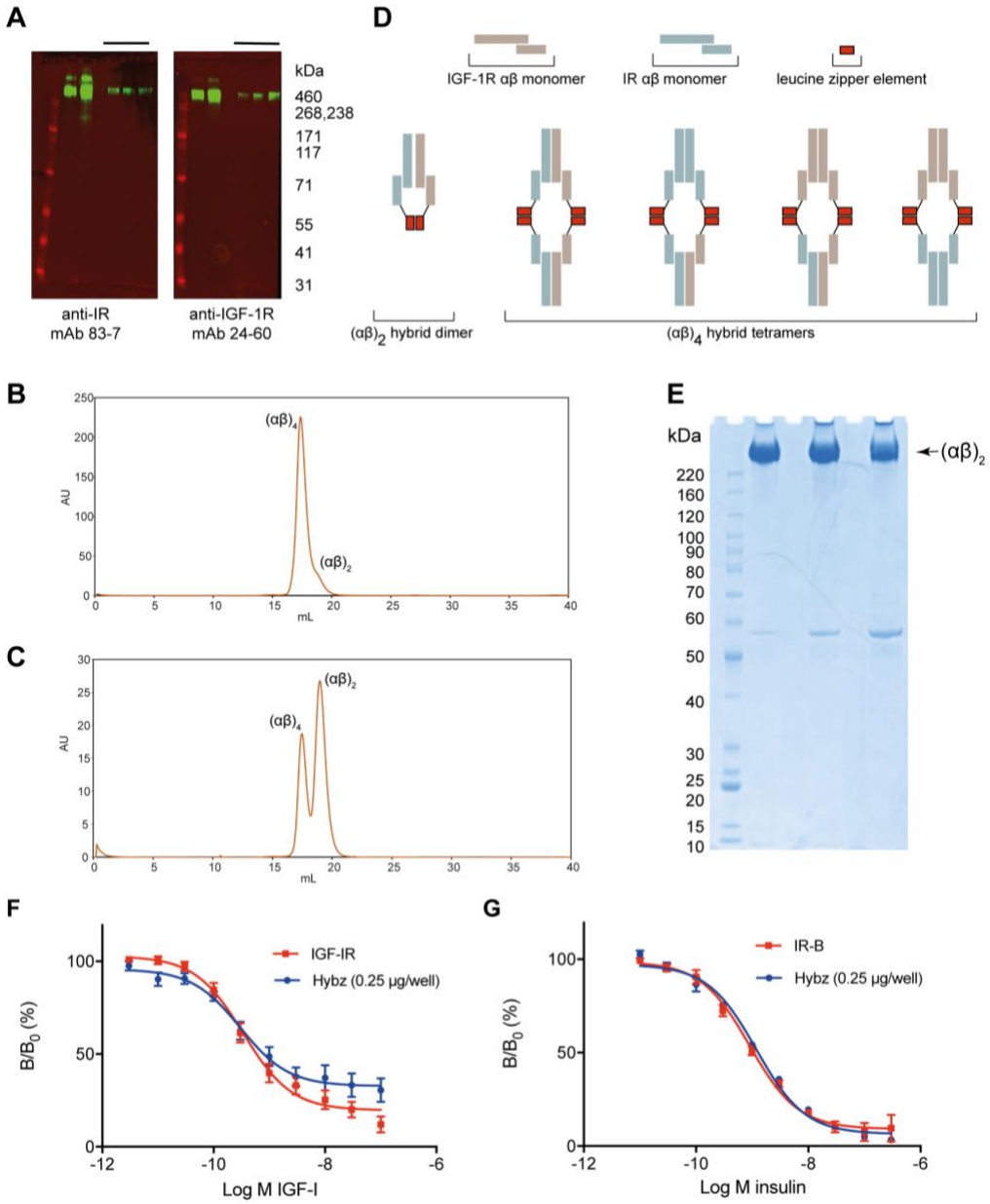

Figure S2. Purification and characterization of HybZip, Related to STAR Methods.

(**A**) Western blots of protein product obtained after serial elution from both 9E10 mAb and 18-44 mAb beads, showing presence of both species in the material (lanes with *bar* on right-hand side of each blot). Left-hand lanes in each blot correspond to pH 3 eluted material obtained from final column wash. Superfluous boundary has been removed from both blot images.

(**B**) Size-exclusion chromatogram obtained from protein product post affinity purification. The dominant peak corresponds to $(\alpha\beta)_4$ species, with a shoulder corresponding to $(\alpha\beta)_2$ species.

(**C**) Enrichment of $(\alpha\beta)_2$ species following re-run of pooled shoulder fractions from (B).

(**D**) Schematic illustrating leucine-zipper cross-linking of receptor ectodomain dimers to form hybrid tetrameric species. All four tetrameric species will be affinity co-purified with the desired hybrid dimer, but can be separated from it by size-exclusion chromatography (see panels B and C).

(**E**) Non-reducing SDS-PAGE gel of pooled $(\alpha\beta)_2$ fractions depicted in (C). Superfluous boundary and blank lanes (to the right) have been removed from the gel image.

(**F**) Competitive displacement assay of labelled IGF-I bound to holo-IGF-1R (*n* = 9) and to HybZip (*n* = 12) by unlabelled IGF-I. Error bars reflect standard error of the mean and are omitted when smaller than marker size. B/B_0 = percentage of binding in the absence of competing ligand.

(**G**) Competitive displacement assay of labelled insulin bound to holo-IR-B (*n* = 9) and to HybZip (*n* = 9) by unlabelled insulin. Error bars reflect standard error of the mean and are omitted when smaller than marker size. B/B_0 = percentage of binding in the absence of competing ligand.

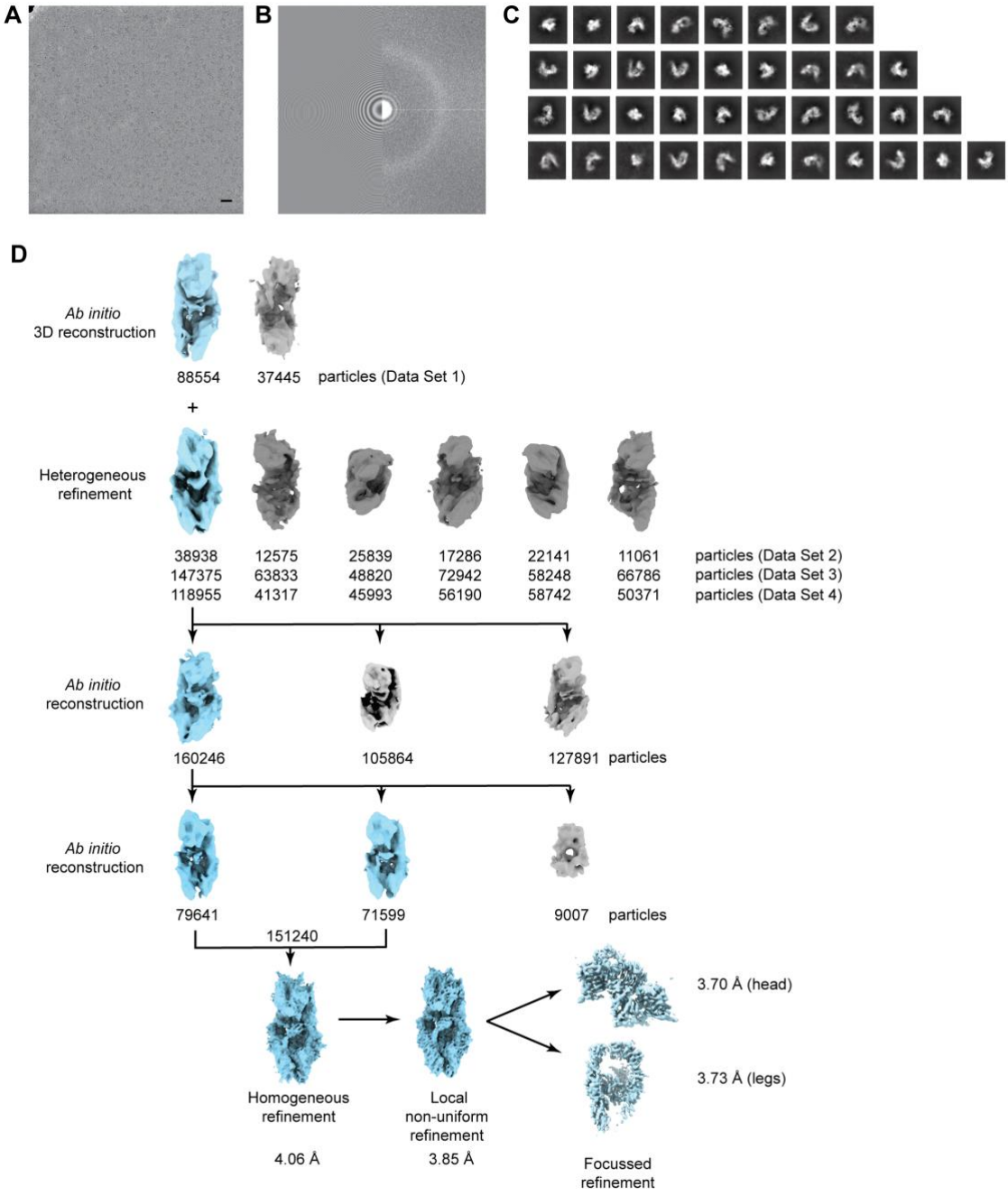

Figure S3. CryoEM reconstruction of IGF-I-complexed HybZip, Related to STAR Methods.

(**A**) Representative image obtained after motion correction (scale bar = 200 Å)

(**B**) Contrast transfer function associated with (A).

(**C**) 2D classes of particles selected from the four data sets (one data set per row; individual class images have been cropped to facilitate enlarged display).

(**D**) Flowchart showing the process of 3D reconstruction of IGF-I-complexed HybZip.

Full details are provided in the **STAR Methods Detail** section.

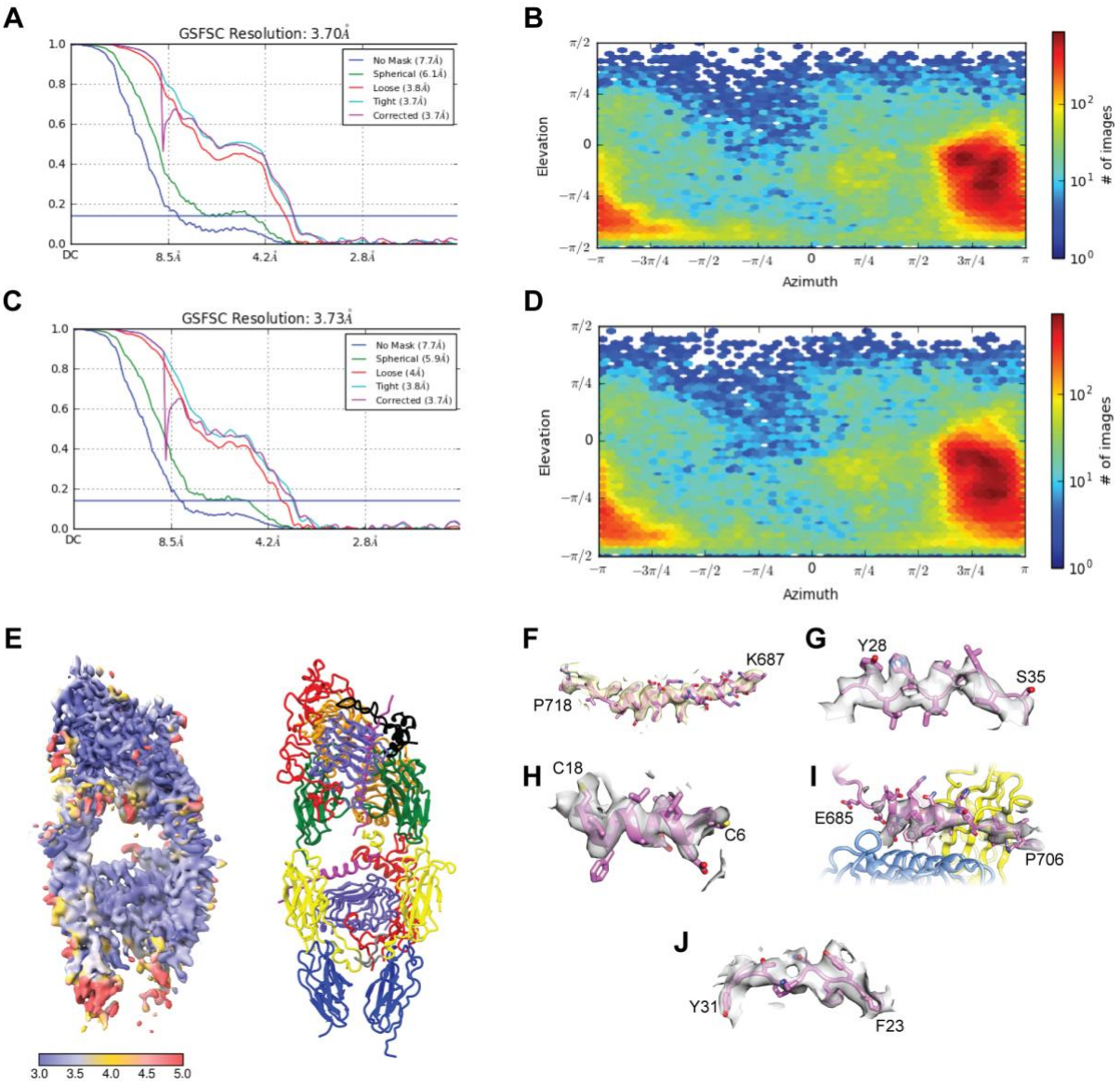

Figure S4. Quality of the 3D reconstructions of the two receptor volumes, Related to STAR Methods.

(**A**),(**C**) Gold-standard Fourier shell correlation (GSFSC) plots for the half-maps associated with the reconstruction of the "head" and "leg" region, respectively, of the IGF-I-complexed HybZip.

(**B**), (**D**) Angular distribution of particles contributing to the reconstruction of the "head" and "leg" region, respectively, of the IGF-I-complexed HybZip.

(**E**) Left panel: overlay of the "head" and "leg" regions maps, colored according to the local resolution. Right panel: ribbon diagram of IGF-I-complexed HybZip, oriented and scaled to match the local-resolution map in the left panel.

(**F**) CryoEM potential density for IR αCT segment, residues Lys687-Pro718. Contour level 0.201, display restricted to within 3.0 Å of depicted residues.

(**G**) CryoEM potential density for IGF-1R domain L1, residues Tyr28-Ser35. Contour level 0.230, display restricted to within 3.0 Å of depicted residues.

(**H**) CryoEM potential density for B domain helix of IGF-I, residues Cys6-Cys18. Contour level 0.242, display restricted to within 3.0 Å of depicted residues.

(**I**) CryoEM potential density for IGF-1R αCT segment, residues Glu685-Pro706. Contour level 0.201, display restricted to within 3.4 Å of depicted residues.

(**J**) CryoEM potential density for C domain of IGF-I, residues Phe23-Tyr31. Contour level 0.160, display restricted to within 3.0 Å of depicted residues.

Table S1. CryoEM data collection parameters, related to STAR METHODS

Data Set:	**1**	**2**	**3**	**4**
Pixel size (Å)	1.06	1.06	1.06	1.06
Dose rate ($e^-.pix^{-1}.sec^{-1}$)	8	6	6	6
Total dose ($e^-.Å^{-2}$)	50	52	52	52
No. frames/movie	36	50	50	50
C_s	2.7	2.7	2.7	2.7
kV	300	300	300	300